

# DISLOCATION DENSITY IN MULTICOMPONENT ALLOYS CoNi, CoFeNi

Somisetty Vaneela

Assistant Professor, Eswar college of Engineering, Narasaraopet

\*\*\*

**Abstract** - Modern alloys have been developed to provide a combination of different properties and balancing the production cost with performance. Conventionally, alloys are processed based on one principal element as a matrix Co-base, Ni-base, Fe-base alloys and with minor additions of other alloying elements to meet the desired properties.

Recently, High entropy alloys (HEAs) have attracted increasing attention because of their composition, microstructures, and adjustable properties. In high entropy alloys there is no principal element and all the elements are taken in equi-atomic proportions, all the elements in HEAs are considered as a solute. Study the dislocation density behavior during mechanical alloying of four different Nano crystalline multicomponent alloys and as cast CoFeNi alloy. The four alloys are being CoNi, CoFeNi.

**Key Words:** Dislocation Alloys, Multi component alloys, Materials, Dislocation Density, CoNi, CoFeNi

## 1. INTRODUCTION

### 1.1 Definition of HEAs:

In principal HEAs are preferentially defined as those alloys containing at least five major elements each having equi-atomic or near equiatomic percentage between 5% to 35% and having high mixing entropy at the liquid state or random state. High mixing entropy can increase the formation of solution type phases that are expected to be stable at elevated temperatures, and in general leads to simpler microstructure. Multi-component HEAs have shown the formation of solid solutions with simple crystal structures having enhanced mechanical properties. Some of these exceptional properties include high temperature strength, thermal stability, oxidation and wear resistance.

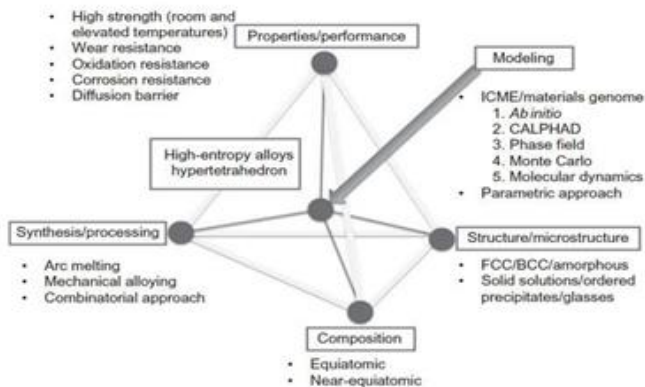


Fig: The materials hyper tetrahedron for HEAs .

### 1.2 Configurational entropy:

Configurational entropy of a given configuration can be evaluated using of the Boltzmann's formula eq. (1) of the statistical thermodynamics [2].

$$\Delta S_{mix} = KB \ln \Omega$$

Where

KB → Boltzmann constant

Ω → The number of microstates

Since, HEAs are equiatomic alloys at its liquid state or regular solid solution state. Its configurational entropy per mole can be calculated by eq.

$$\Delta S_{conf, mix} = R \ln n$$

Where

n → number of elements in HEAs

R → gas constant (8.314 J/K.mol)

HEAs are used as thin films and coatings and as well as composites in some cases. HEAs are said to show these exiting properties due to their four core effects .

### 1.3 Four core effects:

- High entropy effect
- Lattice distortion effect
- Sluggish diffusion
- Cocktail effect

### 1.4 Introduction to Dislocation density:

Dislocations are general feature in crystalline materials. In metals and alloys they are always present. The dislocation density ( $\rho$ ) is a key microstructural parameter since it is strongly related to mechanical properties of metals and alloys.

#### 1.4.1 Definition of Dislocation density:

It is a measure of number of dislocation lines per unit volume of crystalline material. Units of dislocation density is ( $m^{-2}$ )

$$\text{Dislocation density } (\rho) = \frac{\text{Total number of dislocation lines (m)}}{\text{Volume}(m^3)}$$

The dislocation density in metals can be importantly changed during plastic straining, and thermal annealing when they change phase transformations like as the

martensitic transformation found in Fe-C steels. In deformed metals the stored energy offered by the dislocations is the main source for solid state reactions such as recovery and recrystallization. The evaluation of the dislocation density in metals and alloys place a great role in the development of theories of plastic- deformation. Dislocation density can be measured by direct method such as transmission electron microscopy (TEM) and indirect method such as X-ray diffraction (XRD). The direct method can give the microstructural information in small area of the sample, whereas the indirect methods can give average data over a relatively large area exposed to irradiation. The method to evaluate the dislocation density using X-ray diffraction is based on peak broadening analysis.

### 1.5 Peak broadening:

We get the peaks where Bragg's law is satisfied. Ideally the peak should be a sharp line by principle theories, but practically we get broadening of peak.

#### 1.5.1 Major reasons for peak broadening:

1. Instrumental broadening
2. Crystallite size broadening
3. Lattice strain broadening

#### 1. Instrumental broadening:

We have  $n\lambda = 2d \sin \theta$  and d is same for some set of parallel planes but our source is not perfectly characterized, slight variation  $\lambda + \Delta\lambda$  will be there which leads to  $\theta + \Delta\theta$  which is nothing but broadening of peak. Improper alignment of X-ray tube also leads to peak broadening. Sometimes temperature difference also leads to peak broadening.

#### 2. Crystallite size broadening (Bc):

We get peaks for grains where Bragg's law is satisfied, which satisfy extinction rules and note that every grain has some set of planes parallel with respect to surface. Here if completely infinite set of parallel planes, there is complete possibility to get destructive interference completely  $\Delta\theta$  left & right side of Bragg angle. But due to finite set of planes, we won't get completely destructive interference and so, some intensity will occurs at either side of Bragg angle which is nothing but peak broadening.

#### 3. Lattice strain broadening (Bs):

Non -Uniform strain leads to lattice parameter increase or decrease at various positions and causes peak broadening to left & right. Non-uniform strain leads to peak broadening and uniform strain leads to peak shift.

### 1.6 Calculation of crystallite size & lattice strain broadening:

Linear Williamson-Hall equation method eq. 3 is used to calculate total broadening of size and strain [4].

$$B_r = B_c + B_s$$

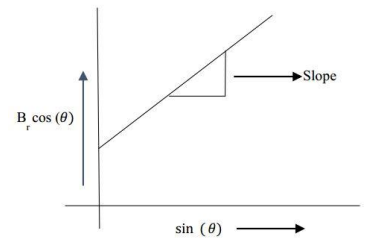
$$B_s = \eta \tan(\theta)$$

From Scherrers formula

$$B_r = \frac{0.9\lambda}{D \cos\theta} + \eta \tan(\theta)$$

$$B_r = \frac{0.9\lambda}{D \cos(\theta)} + \eta \frac{\sin(\theta)}{\cos(\theta)}$$

$$B_r \cos(\theta) = \frac{0.9\lambda}{D} + \eta \sin(\theta) \quad \dots 3$$



$$Y = C + MX$$

where

Slope -  $\eta$  → strain in material

From y-intercept →  $0.9\lambda/D$

D → Crystallite size (nm)

K → Constant ~ 0.9

$\theta$  → Diffraction angle

B → Full width half maximum

B<sub>c</sub> → Crystallite size broadening

B<sub>s</sub> → Lattice strain broadening

The dislocation density ( $\rho$ ) was estimated using the formula of eq. (4), [7] as given by Williamson and Small man method [5, 6].

$$\rho = \frac{2\sqrt{3}(\epsilon_0^2)^{0.5}}{db} \quad \dots 4$$

Where

$\rho$  → Dislocation density (m<sup>-2</sup>)

$(\epsilon_0^2)^{0.5}$  → r.m.s local strain

$(\epsilon_0^2)^{0.5} = \epsilon (2/\pi)$

$\epsilon$  → Lattice strain

d → Crystallite size (nm)

b → Magnitude of the burger's vector

$$b = \frac{a\sqrt{u^2+v^2+w^2}}{2}$$

For fcc metals  $b = (a\sqrt{2}/2)$

## 2. EXPERIMENTAL DETAILS

### 2.1 EXPERIMENT METHODOLOGY

In this chapter, the details for equipment used for material preparation and characterization are presented. A high energy ball milling had been used to prepare the alloys. The structural characterization of the samples is carried out by X-ray diffractometer.

**2.1. Alloy preparation:**

CoNi, CoFeNi, equiatomic alloys were prepared by high energy ball milling. CoFeNi alloy was prepared by casting route. Elements powders weight was calculated by converting atomic percentage into weight percentage.

**Calculations involved:**

CoNi is equiatomic alloy so each element At% is 50%.

CoFeNi is equiatomic alloy so each element At% is 33.3%.

$$Wt\% \text{ of element } A = \frac{\text{Fraction of At\% of } A * \text{Mol. wt of } A}{\sum \text{fraction of At\%} * \text{Mol. wt}}$$

**2.1.1 For Mechanical alloying route:**

For CoNi equiatomic alloy:

**Table 1:**

S.No	Element	At%	Wt.(g)	Wt. of element in 35g
1.	Co	20	50.1017	17.5356
2.	Ni	20	49.8982	17.4644

For CoFeNi equiatomic alloy

**Table 2:**

S.No	Element	At%	Wt.(g)	Wt. of element in 35g
1.	Co	33.33	33.9728	11.8905
2.	Fe	33.33	32.1925	11.2674
3.	Ni	33.33	33.8345	11.8421

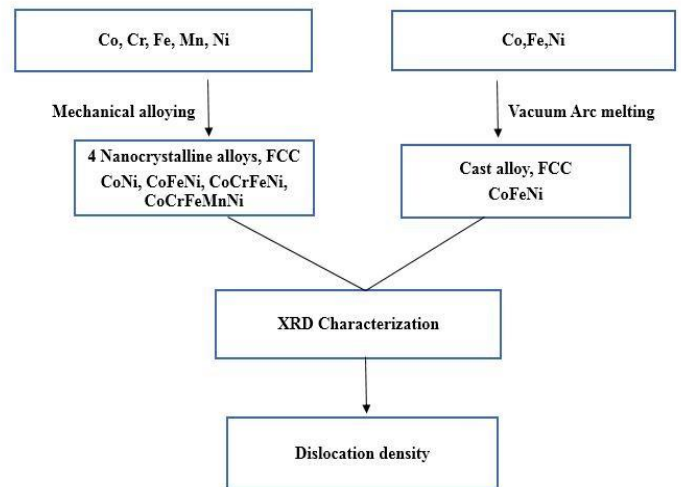
**2.1.2 For casting route:**

For CoFeNi equiatomic alloy

**Table 3:**

S.No	Element	At%	Wt.(g)	Wt. of element in 10g
1.	Co	33.33	33.9730	3.3973
2.	Fe	33.33	32.1930	3.2193
3.	Ni	33.33	33.8350	3.3835

**2.1.3 Experimental flow chart :**



**2.2 PROCESSING OF ALLOYS**

**2.2.1 Mechanical Alloying:**

Mechanical alloying (MA) is a solid state powder processing technique involving repeated welding, fracturing and rewelding of powder particles in a high energy ball milling, in which elemental blends are milled to gain alloying in the atomic level [8]. It is a non-equilibrium process. In addition to elemental blends, pre alloyed powders and ceramics, such as oxides, nitrides, etc. can also be used to produce alloys and composites by this technique. MA is very popular for the synthesis of oxide dispersed steels, which were used for high temperature structural applications [9].

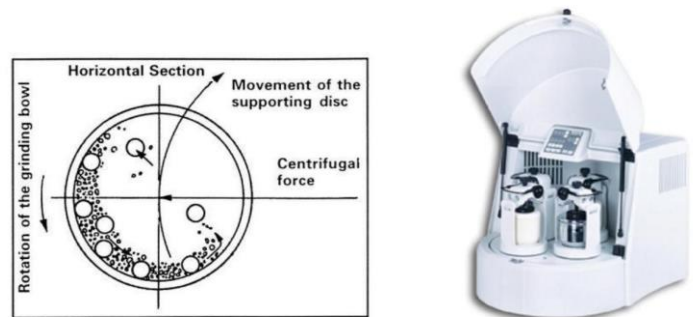


Fig: Ball and powder moment in MA, Planetary ball mill unit

The elemental blends of Co, Cr, Fe, Mn, and Ni were ball milled using planetary ball mill (Fritsch Pulversitte -5, Germany). Here type of ball milling is wet type milling. The milling media (vials and balls) were tungsten carbide and a balls to powder ratio of 10:1 was maintained in medium of toluene as process control agent. Each vial was used to alloy 35 grams of powder with 350 grams of tungsten carbide ball. The milling was performed at 300 rpm for 15 hours. The powder samples were taken out at an interval of 2 hours to analyze the microstructural evolution during milling using XRD characterization.

### 2.2.2 Vacuum Arc Melting:

Another CoFeNi equi-atomic cast alloy was planned to prepare through Vacuum arc melting to compare the dislocation density of cast alloy with mechanically alloyed alloys. Vacuum arc melting is mainly used for melting of metals typically to form alloys [8]. Here a standard Tungsten Inert Gas (TIG) welding unit is used for power source. Heat was produced by the electric arc struck between the metals and electrode for melt the metals which are placed in the crucible to form an alloy in the copper hearth.

In vacuum arc melting the heating chamber is evacuated and then immediately filled with argon gas. Creating vacuum or evacuation of the chamber prevent the oxidation of the melt. Repeated melting is carried out to give better the homogeneity (uniform composition) of the alloy.

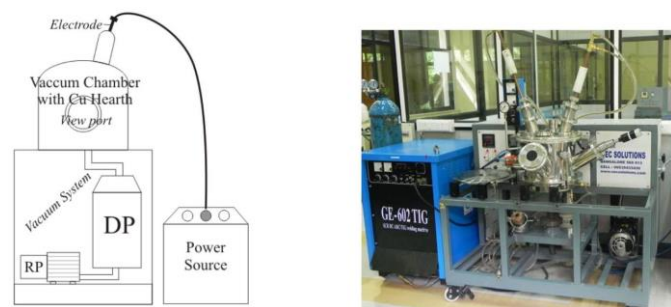


Fig 5: Schematic of the arc melting system, Arc melting unit

The vacuum arc melting was carried out in a titanium guttered argon atmosphere prepared after evacuation up to a vacuum pressure of  $10^5$  mbar. A thoriated tungsten electrode was used to melt the alloys in a water cooled copper mould. The alloy was planned to be remelted four times to achieve homogeneity.

### 2.2.3 X-ray Diffraction:

X-ray diffraction is one of the powerful technique tools during the last two decades for materials characterization since its discovery by Roentgen in 1895. By comparing the positions and intensities of the diffraction peaks against a library of known crystalline materials, the target material can be identified. In addition, multiple phases in a sample can be identified. For single phase materials the crystal structure can be obtained directly using X-ray diffraction [4].

The XRD characterization was done using X'pert Pro (PANalytical, The Netherlands) X-ray diffract meter in Bragg-Brentano geometry equipped with X'Celerator detector with Cu  $K\alpha$  radiation (45 kV, 30 mA). A flat stage sample holder was used for all XRD analyses at room temperature. XRD measurements were performed in a range of  $20^\circ$  to  $90^\circ$  using  $0.02^\circ$  step size with a 20 seconds time per step. The microstructural analysis (crystallite size, lattice strain, lattice parameter) was done after fitting the XRD pattern using Pseudo-Voigt function in High score plus software [7].



Fig: X-ray diffract meter

The most intense peak of the phase under study was fitted as a Pseudo-Voigt function to deconvolute Lorentzian or Cauchy broadening and Gaussian broadening. The method presumes a Gaussian profile shape for lattice strain contributions, a Lorentzian profile shape for the crystallite size contributions and a Voigt shape for sum profile. Silicon was used as a standard for the removal of instrumental broadening. Each XRD pattern was repeated thrice, crystallite size and lattice strain were calculated to introduce an error marker for every reading.

## RESULTS AND DISCUSSIONS

### Mechanical alloying route:

#### 3.1 CoNi (MA) equiatomic alloy:

This alloy is formed by milling equiatomic powders of Co and Ni for 10 hours. XRD pattern in Fig 8 illustrate the phase formation behavior of CoNi alloy during mechanical alloying.

Individual elemental diffraction peaks that appeared at the beginning of milling, evolve into diffraction peaks corresponds to FCC phase for CoNi system after 10 h milling. The (111) high intensity peak of FCC phase was chosen to illustrate the phase analysis during milling. The peaks were deconvoluted to identify the phases and their contributions to the intensity. The evolution of FCC phase can be attributed to the presence of strong FCC forming element such as Ni in CoNi system. Decrease in the high intensity peak of Co after 4h of a milling is a clear indication that Co dissolves into FCC lattice of Ni to form Co-Ni solid solution. It can be inferred that FCC phase evolves by dissolution of Co into Ni lattice. After 8 h of milling the Co peak disappears completely, whereas the remaining peaks become more symmetric (i.e., the FCC (111) peak, shows in the fig 8. That means, there is complete alloying in case of 10:1 BPR for 10 h of milling.

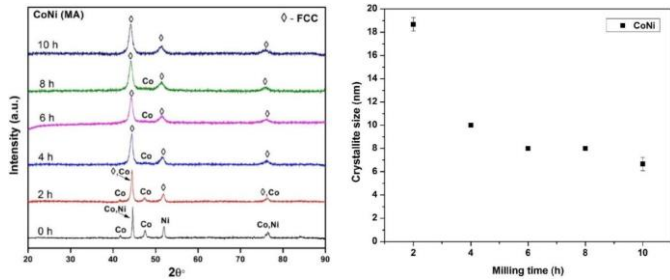


Fig 8: X-ray diffraction patterns of CoNi samples as a function of the milling time.

Fig 9: Milling time dependence of the crystallite size for the mechanical alloyed CoNi powders at room temperature.

Table: Microstructural evolution (crystallite size, lattice strain, dislocation density) during ball milling.

BPR 10:1, 300 rpm			
Milling time (h)	crystallite size d (nm)	Lattice strain (%)	Dislocation density ( $\times 10^{15} \text{ m}^{-2}$ )
2	18.6 ( $\pm 0.5$ )	-0.06 ( $\pm 0.00$ )	—
4	10 ( $\pm 0.0$ )	0.24 ( $\pm 0.02$ )	2.69
6	8 ( $\pm 0.0$ )	0.20 ( $\pm 0.04$ )	2.85
8	8 ( $\pm 0.0$ )	0.26 ( $\pm 0.02$ )	3.58
10	6.6 ( $\pm 0.5$ )	-0.05 ( $\pm 0.00$ )	—

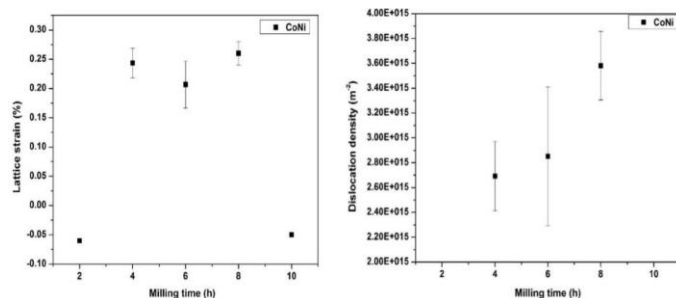


Fig 10: Milling time dependence of the lattice strain, dislocation density for the mechanical alloyed CoNi powders at room temperature.

The crystallite size of FCC phase and lattice strain was employed using Linear Williamson hall method due to its simplistic approach path. Fig 9.shows the dependence of the calculated grain size on the milling time. It is seen that the average crystallite size decreases exponentially in the initial hours of milling to reach a nearly constant value of 8 nm after 6 h of milling [10].

Fig10 (a).shows the dependence of the calculated lattice strain and dislocation density on the milling time. The drastic decrease of the grain size matched to substantial increase of lattice strain from 0.06% to 0.26% for 2h and 8h of milling

respectively. Here we note a decrease of lattice strain for 6h of milling (fig.10 (a)) and can be attributed to strain release. This is most probably due to dynamic recrystallization of grains created by local heating during the mechanical alloying process. Lattice strain caused by MA is commonly attributed to the generation and movement of dislocations [11]. Fecht [12] asserted that generation and movement of dislocations could decrease grain size. The final grain size of the FCC solid solution after 10h of milling is about 7nm. The calculated dislocation densities of the MA CoNi samples are represented in Fig10 (b). It is clearly seen that dislocation density increases from about  $2.69 \times 10^{15} \text{ m}^{-2}$  to  $3.58 \times 10^{15} \text{ m}^{-2}$  with increasing milling time from 4h to 8h.

### 3.2 CoFeNi (MA) equiatomic alloy:

This alloy is formed by milling equiatomic powders of Co, Fe and Ni for 10 hours. XRD pattern in Fig.11 illustrate the phase formation behavior of CoFeNi alloy during mechanical alloying. Individual elemental diffraction peaks that appeared at the beginning of milling, evolve into diffraction peaks corresponds to FCC phase for CoFeNi system after 10 h milling. The (111) high intensity peak of FCC phase was chosen to illustrate the phase analysis during milling. The peaks were deconvoluted to identify the phases and their contributions to the intensity.

The evolution of FCC phase can be attributed to the presence of strong FCC forming element such as Fe and Ni in CoFeNi system. Decrease in the high intensity peak of Co after 4h of a milling is a clear indication that Co dissolves into FCC lattice of Ni to form CoFeNi solid solution. It can be inferred that FCC phase evolves by dissolution of Co and Fe into Ni lattice. As milling progresses up to 8h the BCC phase is decreasing and results in a major amount of FCC phase and small amount of BCC phase is present (fig ). After 6 h of milling the Co peak disappears completely, whereas the remaining peaks become more symmetric (i.e., the FCC (111) peak, shows in the fig.11. That means, there is complete alloying in case of 10:1 BPR for 10 h of milling.

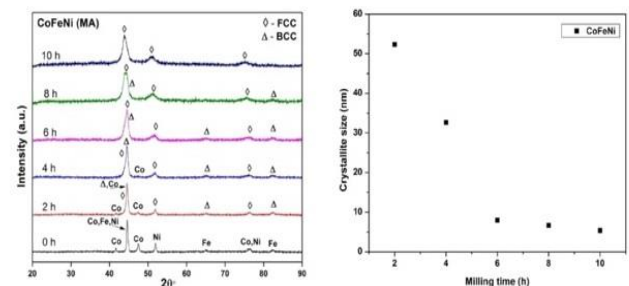
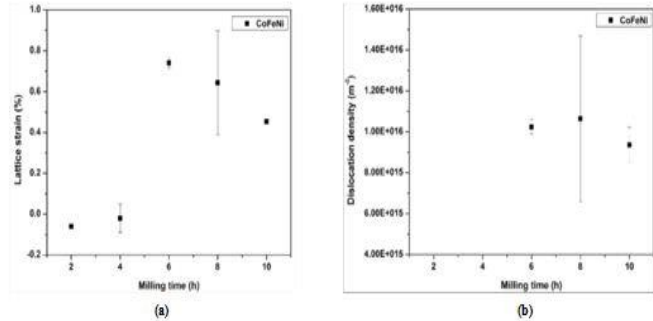


Fig : X-ray diffraction patterns of CoFeNi samples as a function of the milling time.

Fig : Milling time dependence of the crystallite size for the mechanical alloyed powders at room temperature.

The crystallite size of FCC phase and lattice strain was employed using Linear Williamson hall method due to its simplistic approach. Fig.12 shows the dependence of the

calculated grain size on the milling time. It is seen that the average crystallite size decreases exponentially in the initial hours of milling to reach a nearly constant value of 8 nm after 6 h of milling. The final grain size of the FCC solid solution after 10h of milling is about 5nm [10].



**Fig:** Milling time dependence of the lattice strain, dislocation density for the mechanical alloyed CoFeNi powders at room temperature.

**Table:** Microstructural evolution (crystallite size, lattice strain, dislocation density) during ball milling.

BPR 10:1, 300 rpm			
Milling time (h)	crystallite size d (nm)	Lattice strain (%)	Dislocation density (x 10 <sup>16</sup> m <sup>-2</sup> )
2	52.3 (± 0.5)	-0.06(±0.00)	-
4	32.6 (± 0.5)	-0.02 (± 0.06)	-
6	8 (± 0.0)	0.74 (± 0.02)	1.02
8	6.6 (± 0.5)	0.64 (± 0.25)	1.06
10	5.3 (± 0.5)	0.45 (± 0.01)	0.93

Fig.13 (a): shows the dependence of the calculated lattice strain and dislocation density on the milling time. The drastic decrease of the grain size matched to substantial increase of lattice strain from 0.02% to 0.74% for 4h and 6h of milling respectively. Here we note a decrease of lattice strain for 8h and 10h of milling (fig.13(a)) and can be attributed to strain release. This is most probably due to dynamic recrystallization of grains created by local heating during the mechanical alloying process. Lattice strain caused by MA is commonly attributed to the generation and movement of dislocations [11]. Fecht [12] asserted that generation and movement of dislocations could decrease grain size.

The calculated dislocation densities of the MA CoFeNi samples are represented in fig.13 (b). It is clearly seen that dislocation density increases from about 1.02 x 10<sup>16</sup>m<sup>-2</sup> to 1.06 x 10<sup>16</sup>m<sup>-2</sup> with increasing milling time from 6h to 8h and then decreases to 0.93 x 10<sup>16</sup>m<sup>-2</sup> for 10h of milling.

#### 4. REFERENCES

- [1] High Entropy Alloys by B .S. Murty et.al., (2014).
- [2] Porter, A., H. David and K.E. Easterling, Van Nostrand Reinhold Co Ltd. (1981).
- [3]R. A .Renzetti, H.R .Z.Sandhin, R.E. Bolmaro, P.A. Suzuki and A. Moslang, Materials Science and Engineering A 534 (2012) 142-146.